ELSEVIER

Journal of Contaminant Hydrology 49 (2001) 173–199

JOURNAL OF Contaminant Hydrology

www.elsevier.com/locate/jconhyd

A novel two-dimensional model for colloid transport in physically and geochemically heterogeneous porous media

Ning Sun [a], Menachem Elimelech [a,*], Ne-Zheng Sun [b], Joseph N. Ryan [c]

[a] *Environmental Engineering Program, Department of Chemical Engineering, Yale University, P.O.Box 208286, New Haven, CT 06520-8286, USA*

[b] *Department of Civil and Environmental Engineering, University of California, Los Angeles, Los Angeles, CA 90095, USA*

[c] *Department of Civil, Environmental, and Architectural Engineering, University of Colorado, Boulder, CO 80203, USA*

Received 11 January 2000; received in revised form 20 July 2000; accepted 10 November 2000

Abstract

A two-dimensional model for colloid transport in geochemically and physically heterogeneous porous media is presented. The model considers patchwise geochemical heterogeneity, which is suitable to describe the chemical variability of many surficial aquifers with ferric oxyhydroxide-coated porous matrix, as well as spatial variability of hydraulic conductivity, which results in heterogeneous flow field. The model is comprised of a transient fluid flow equation, a transient colloid transport equation, and an equation for the dynamics of colloid deposition and release. Numerical simulations were carried out with the model to investigate the colloid transport behavior in layered and randomly heterogeneous porous media. Results demonstrate that physical and geochemical heterogeneities markedly affect the colloid transport behavior. Layered physical or geochemical heterogeneity can result in distinct preferential flow paths of colloidal particles. Furthermore, the combined effect of layered physical and geochemical heterogeneity may result in enhanced or reduced preferential flow of colloids. Random distribution of physical heterogeneity (hydraulic conductivity) results in a random flow field and an irregularly distributed colloid concentration profile in the porous medium. Contrary to random physical heterogeneity, the effect of random patchwise geochemical heterogeneity on colloid transport behavior is not significant. It

* Corresponding author. Tel.: +1-203-432-7289.
E-mail address: menachem.elimelech@yale.edu (M. Elimelech).

PII: S0169-7722(00)00193-5

is mostly the mean value of geochemical heterogeneity rather than its distribution that governs the colloid transport behavior.

Keywords: Colloid transport; Physical heterogeneity; Geochemical heterogeneity; Porous media; Colloid-facilitated transport; Colloid deposition; Patchwise geochemical heterogeneity; Ferric oxyhydroxide coating

1. Introduction

It is now widely accepted that mobile subsurface colloids can facilitate the transport of strongly-sorbing contaminants (McCarthy and Zachara, 1989; Ryan and Elimelech, 1996; Grolimund et al., 1996; Roy and Dzombak, 1998). In many other cases, colloidal particles, such as pathogenic bacteria and viruses, are contaminants themselves (Yates et al., 1985; Harvey et al., 1989). To accurately assess the transport and fate of such contaminants in groundwater, detailed yet realistic models for colloid transport in subsurface porous media are needed.

Several models for colloid transport in granular porous media have been developed. Corapcioglu and Jiang (1993) developed a one-dimensional model to describe colloid transport in homogeneous porous media, with both colloid deposition and release modeled as first-order kinetics processes. Johnson and Elimelech (1995) incorporated linear (Langmuirian) and nonlinear (random sequential adsorption) particle deposition dynamics in colloid transport modeling to account for the phenomenon of blocking. Saiers et al. (1994) used both first- and second-order (blocking) kinetics approaches to model the transport and deposition of colloidal anatase, boehmite, and silica in packed-sand columns. Song and Elimelech (1994) considered the effect of surface charge (geochemical) heterogeneity on colloid deposition and transport, with the surface charge heterogeneity being modeled as either random microscopic sites or as patches. In a later study, Johnson et al. (1996) incorporated both patchwise geochemical heterogeneity and random sequential deposition dynamics in a one-dimensional colloid transport model. Their model predictions were in good agreement with experimental silica colloid breakthrough curves through a column packed with geochemically heterogeneous sand grains.

To date, most available models for colloid transport, including the models mentioned in the previous paragraph, consider only physically homogeneous porous media. Subsurface porous media, however, are known to be physically heterogeneous (e.g., LeBlanc et al. 1991; Hess et al., 1992; Dagan, 1989). Among the few attempts to consider effects of physical heterogeneity on colloidal transport, Abdel-Salam and Chrysikopoulos (1995) and Chrysikopoulos and Abdel-Salam (1997) modeled colloid transport in a fractured-rock matrix with spatially variable aperture. Saiers et al. (1994) carried out colloid transport experiments in a structured-heterogeneous porous medium. In their experiments, the column was packed with concentric layers of homogeneous sand of different grain size, aligned parallel to the flow direction. The results of both studies showed that physical heterogeneity of porous media significantly influences colloidal transport behavior.

The previously described models for colloid transport in geochemically heterogeneous porous media dealt only with porous media surfaces having a constant geochemi-

cal heterogeneity. However, a spatially distributed geochemical heterogeneity is very likely to exist in the subsurface environment due to the inherent geochemical variability of subsurface geological formations. Thus, it is imperative that the recent colloid transport modeling approaches be extended to incorporate the more realistic spatial distribution of geochemical heterogeneity.

In this paper, we develop a two-dimensional colloid transport model for physically as well as geochemically heterogeneous porous media. In this model, the colloid transport equation is coupled with the fluid flow equation. Patchwise geochemical heterogeneity and nonlinear dynamics of particle deposition and release are considered as the main mechanisms governing colloid transfer between the immobile solid phase of the porous medium and the mobile colloidal phase. Layered or random distributions of hydraulic conductivity are introduced into the flow equation to describe the physically heterogeneous porous media. Constant or spatially distributed geochemical patches are incorporated in the colloid deposition and release equation to represent the geochemical heterogeneity of the porous matrix surfaces. A variant of a finite element method—the multiple cell balance (MCB)—is used to obtain a numerical solution of the proposed model. The model is used to carry out a systematic numerical investigation on the influence of physical and geochemical heterogeneities on colloidal transport in subsurface porous media.

2. Model development

We consider a confined aquifer where the fluid is in laminar motion and the suspended colloidal particles travel with the fluid. The colloidal particles are assumed to be Brownian (i.e., less than about 1 μm) and monodisperse. Spatial distributions of the physical and geochemical heterogeneities of the subsurface porous medium are rigorously incorporated in the model.

2.1. Flow field

The transient flow equation for a fluid in a confined subsurface porous medium, such as a confined groundwater aquifer, is usually written as (Bear, 1972; de Marsily, 1986)

$$S_s \frac{\partial h}{\partial t} = \nabla \cdot (\mathbf{K} \nabla h) - Q, \tag{2.1}$$

where h is the hydraulic head, t is the time, S_s is the specific storage, $\mathbf{K}$ is the hydraulic conductivity, and Q is the pumping or recharge rate. Under natural gradient flow conditions, the fluid is usually in steady state flow. Hence, the spatially distributed hydraulic heads are determined for steady-state flow field and then used to calculate the fluid velocity by applying Darcy's law:

$$\mathbf{q} = -\mathbf{K} \nabla h, \tag{2.2}$$

where ∇h is the hydraulic head gradient and $\mathbf{q}$ is Darcy's velocity. The average pore velocity (V), which usually appears in the transport equation, is the ratio of Darcy's velocity to porosity (ε).

2.2. Physical heterogeneity of subsurface porous media

The spatial variation of hydraulic conductivity results in heterogeneous flow field that influences colloid transport and the resulting particle concentration distribution in the porous medium. Two types of physical heterogeneity are investigated: layered heterogeneity and random heterogeneity.

In a layered, physically heterogeneous subsurface porous medium, the medium is made up of several homogeneous layers. Thus, while each layer is homogeneous (i.e., with constant hydraulic conductivity), the entire system is heterogeneous. For instance, porous media with fractures (Ibaraki and Sudicky, 1995a,b) or large blocks of macropores may be described as layered heterogeneous.

Substantial progress has been made in the past two decades to understand the random physical heterogeneity of groundwater aquifers. Evidence from field-scale hydraulic conductivity measurements indicates that the spatial distribution of hydraulic conductivity is lognormal (e.g., Freeze, 1975; Sudicky, 1986; Hess, 1989). It was also found that there exists a non-Gaussian behavior of the log-transformed hydraulic conductivity at relatively small scales, and that this non-Gaussian behavior shifts to Gaussian behavior as the length scale increases (e.g., Painter, 1996; Liu and Molz, 1997). Because of lack of knowledge on this transition length scale and the fact that lognormally distributed hydraulic conductivity has been used by many hydrologists (e.g., Gelhar et al., 1979; Gelhar and Axness, 1983; Dagan, 1989; Rubin, 1990), a lognormal distribution is adopted here to describe the random spatial variation of hydraulic conductivity.

Let $Y = \ln K$, with a constant mean m_Y and variance σ_Y^2. The covariance function of Y is assumed to have an isotropic exponential form,

$$C_Y(\mathbf{r}) = \sigma_Y^2 \exp\left(-\frac{|\boldsymbol{r}_Y|}{l_Y}\right), \tag{2.3}$$

where $\boldsymbol{r}_Y$ is the planar distance vector between two positions in the heterogeneous domain and l_Y is the integral scale of Y. Using the statistical properties of spatial distribution, the random field of hydraulic conductivity can be generated by the turning band method (Mantoglou and Wilson, 1982; Tompson et al., 1989).

2.3. Geochemical heterogeneity of subsurface porous media

Ferric oxyhydroxide coatings are the main source of geochemical heterogeneity of the solid matrix in many surficial aquifers containing iron-bearing minerals (e.g., Fuhs et al., 1985; Scholl et al., 1990; Scholl and Harvey, 1992; Coston et al., 1995; Zachara et al., 1995; Ryan et al., 1999). These coatings on mineral grain surfaces provide favorable sites (area) for colloid deposition because they are positively charged whereas the majority of subsurface colloidal particles are negatively charged. Here, we adopt the patch model (Song et al., 1994) to describe the geochemical heterogeneity of subsurface porous media. The model is characterized by the heterogeneity parameter, λ, which is defined as the ratio of the surface area favorable for deposition (i.e., particle deposition

onto this area is not hindered by colloidal interactions and is transport limited) to the total interstitial surface area over a representative elementary volume (REV) of a porous medium. Note that colloid deposition or release can occur on both the favorable (λ) and unfavorable ($1-\lambda$) fractions, albeit at much different rates.

Because the chemical composition of subsurface minerals and solution chemistry vary spatially in subsurface aquatic environments, the geochemical heterogeneity, defined over an REV, may vary significantly throughout the subsurface porous medium. The geochemical heterogeneity of a porous medium can be assumed to be constant over the entire porous medium, or to have different values at different locations in the porous medium. Accordingly, two spatial variations of geochemical heterogeneity are considered: layered geochemical heterogeneity and random geochemical heterogeneity.

Compared to layered geochemical heterogeneity, detailed statistical information on the chemical properties of the subsurface porous medium is needed to model random geochemical heterogeneity. To date, there are no reported studies on the random field of geochemical heterogeneity of subsurface porous media in relevance to colloid transport. Several studies on solute transport in heterogeneous porous media have described the variation of solute sorption coefficients by a normal distribution (e.g., Black and Freyberg, 1987; Chrysikopoulos et al., 1990; Bosma and van der Zee, 1993). Although solute transport behavior is quite different than colloidal transport behavior, we adopt a similar approach and describe the random field of geochemical heterogeneity as normally distributed with a constant mean $E(\lambda)$ and a variance σ_λ^2. The turning band method (Mantoglou and Wilson, 1982; Tompson et al., 1989) is used to generate the realization of the two-dimensional random field of normally distributed geochemical heterogeneity, with a first-order exponential autocorrelation function:

$$C_\lambda(\mathbf{r}) = \sigma_\lambda^2 \exp\left(-\frac{|\mathbf{r}_\lambda|}{l_\lambda}\right), \tag{2.4}$$

where l_λ is the integral scale of λ.

The mean value of the geochemical heterogeneity λ in surficial aquifers with Fe oxyhydroxide coatings is thought to be small, on the order of a few percent (Heron et al., 1994; Coston et al., 1995; Ryan et al., 1999). With a mean value of only a few percent, a normal distribution cannot well describe the portion of the relatively large geochemical heterogeneity values, which possibly exist in natural systems. Thus, in addition to normal distribution, a lognormal distribution will be used when significant variations of geochemical heterogeneity, with a small mean value of only a few percent, are desired.

2.4. Colloid transport equation

The colloid transport equation can be derived from mass balance of colloids over an REV of a porous medium. There are three main mechanisms controlling colloid transport: hydrodynamic dispersion, advection, and colloid transfer between the stationary solid matrix and the mobile colloidal phase through colloid deposition and release.

These mechanisms can be described by the generalized advection–dispersion equation (de Marsily, 1986):

$$\frac{\partial C}{\partial t} = \nabla \cdot (\mathbf{D}\nabla C) - \nabla \cdot (\mathbf{V}C) - \frac{\rho_b}{\varepsilon}\frac{\partial S}{\partial t}, \tag{2.5}$$

where C is the mass concentration of colloids in the aqueous phase, S is the ratio of the colloid mass captured by the solid matrix to the total mass of solid matrix, $\mathbf{D}$ is the particle hydrodynamic dispersion tensor, $\boldsymbol{V}$ is the particle velocity vector, ε is the porosity of the porous medium, and ρ_b is the bulk density of the porous medium.

Because the average pore radius in sandy aquifers is quite large compared to the size of Brownian (submicrometer size) colloidal particles, size exclusion effects are not considered. Thus, the particle velocity and interstitial fluid velocity are assumed to be equal. For the two-dimensional transport problem considered here, the components of the hydrodynamic dispersion coefficient are related to the particle Stokes–Einstein diffusivity D_d and the components of the interstitial velocity ($\overline{V}_i$ and $\overline{V}_j$) by

$$D_{ij} = \alpha_T \overline{V}\delta_{ij} + (\alpha_L - \alpha_T)\frac{\overline{V}_i\overline{V}_j}{\overline{V}} + D_d T\delta_{ij}, \tag{2.6}$$

where α_L and α_T are the longitudinal and transverse dispersivities, respectively, T is the porous medium tortuosity, δ_{ij} is the Kronecker delta, and $\overline{V}$ is the geometric average of $\overline{V}_i$ and $\overline{V}_j$. Note that in this study a unidirectional flow along the x direction is assumed with $\overline{V}_j = 0$.

To appropriately describe the dynamic aspects of colloid deposition and the associated blocking effects, the colloid transport equation is expressed in terms of particle number concentration rather than mass concentration (Johnson et al., 1996),

$$\frac{\partial n}{\partial t} = \nabla \cdot (\mathbf{D}\nabla n) - \nabla \cdot (\mathbf{V}n) - \frac{f}{\pi a_p^2}\frac{\partial \theta}{\partial t}, \tag{2.7}$$

where n is the number concentration of colloids, θ is the fractional surface coverage, defined as the total cross-section area of deposited colloids per interstitial surface area of the porous medium solid matrix, f is the specific surface area (i.e., interstitial surface area per porous medium pore volume), and a_p is the radius of colloidal particles. It can be readily shown that Eq. (2.7) is equivalent to Eq. (2.5).

2.5. Colloid deposition and release

Using the patchwise model for geochemical heterogeneity, the particle surface coverage rate of mineral grains is given by (Johnson et al., 1996)

$$\frac{\partial \theta}{\partial t} = \lambda\frac{\partial \theta_f}{\partial t} + (1-\lambda)\frac{\partial \theta_u}{\partial t}. \tag{2.8}$$

When considering the dynamic aspects of particle deposition and release, the rate equations corresponding to the favorable and unfavorable surface fractions can be expressed as

$$\frac{\partial \theta_f}{\partial t} = \pi a_p^2 k_{dep,f} n B(\theta_f) - k_{det,f} \theta_f R(\theta_f), \tag{2.9a}$$

$$\frac{\partial \theta_u}{\partial t} = \pi a_p^2 k_{dep,u} n B(\theta_u) - k_{det,u} \theta_u R(\theta_u), \tag{2.9b}$$

where the subscripts f and u represent the favorable (λ) and unfavorable ($1-\lambda$) REV surface fractions, respectively, k_{dep} is the colloid deposition rate constant, k_{det} is the colloid release rate constant, and $B(\theta)$ and $R(\theta)$ are the dynamic blocking and release functions, respectively. The colloid deposition rate coefficient is related to the single collector efficiency η commonly used in filtration theories by (Johnson and Elimelech, 1995)

$$k_{dep} = \frac{\eta \varepsilon V}{4} = \frac{\alpha \eta_0 \varepsilon V}{4}, \tag{2.10}$$

where V is the colloid (or fluid) advection velocity, ε is the porosity of the porous medium, α is the attachment (collision) efficiency, and η_0 is the favorable single collector removal efficiency.

The dynamic blocking function $B(\theta)$ characterizes the probability of colloid deposition by quantifying the fraction of collector surface still available for deposition of colloids (Johnson and Elimelech, 1995). It accounts for the blocking effect of deposited colloids on the particle deposition rate. Two types of dynamic blocking functions are generally recognized: the Langmuirian dynamic blocking function and the random sequential adsorption (RSA) dynamic blocking function. Recent experimental investigations have shown that the RSA model describes the dynamics of particle deposition in porous media better than the conventional Langmuirian model (Johnson and Elimelech, 1995; Johnson et al., 1996).

The general form of the RSA dynamic blocking function is

$$B(\theta) = 1 - a_1\left(\frac{\theta}{\theta_{max}}\right) + a_2\left(\frac{\theta}{\theta_{max}}\right)^2 + a_3\left(\frac{\theta}{\theta_{max}}\right)^3, \tag{2.11}$$

where θ_{max} is the maximum attainable surface coverage, and a_1, a_2, and a_3 are coefficients that can be evaluated theoretically (for ideal particles and collector surfaces and simple flow conditions) or empirically. The coefficients used by Johnson and Elimelech (1995) for $B(\theta)$ will be used in this colloid transport model as they were found adequate to describe the dynamics of blocking in flow of monodisperse latex microspheres in columns packed with spherical uniform glass beads.

Because colloid deposition onto the favorable surface fraction is usually irreversible (particles and patch surfaces are oppositely charged), the RSA model can be used to describe the dynamics of particle deposition onto the favorable surface fraction. A similar dynamic blocking function was also chosen to describe the blocking of the unfavorable fraction, although the deposition onto the unfavorable surface fraction was

assumed to be reversible. This assumption, however, has negligible effect on the colloid transport behavior since the deposition rate on the unfavorable surface fraction is much smaller than that on the favorable fraction, and the maximum surface coverage for the unfavorable surface fraction is much smaller than that on the favorable surface fraction.

The dynamic release function describes the probability of colloid release from porous media surfaces covered by retained colloids, somewhat analogous to the dynamic blocking function. In principle, this function should depend on the colloid residence time and the retained colloid concentration (Meinders et al., 1992; Johnson et al., 1995). When $R(\theta)=1$, the release terms in Eqs. (2.9a, 2.9b) represent a first-order kinetics release mechanism. Because the mechanisms of colloid release are relatively not well understood at the present time, only a first-order release rate will be considered in this paper.

2.6. Correlation between physical heterogeneity and colloid deposition rate

In modeling colloid transport, the variation of flow field will change the colloid concentration distribution in the studied domain not only by affecting hydrodynamic dispersion and advection, but also by influencing the colloid deposition rate. For Brownian colloids, whose deposition rate is controlled by a convective–diffusive mechanism, there exists a positive relationship between the hydraulic conductivity and the particle deposition rate. Based on Eq. (2.10), the colloid deposition rate (k_{dep}) is proportional to ($\eta_0 V$), with η_0 for Brownian colloids being proportional to $V^{-2/3}$ (Levich, 1962; Elimelech and O'Melia, 1990). Combining this relationship with Darcy's law, one obtains that the colloid deposition rate (k_{dep}) is proportional to $K^{1/3}$. A consequence of this relationship is that a random field of hydraulic conductivity leads to a random field of colloid deposition rate as well.

We assume that $P=\ln k_{\mathrm{dep}}$ is normally distributed with a mean $\langle P\rangle$ and variance σ_P^2, and has a similar form of the covariance function as the hydraulic conductivity field. To describe the correlation between the random hydraulic conductivity field and the colloid deposition rate, it is further assumed that

$$P=\langle P\rangle+\omega P'+\gamma Y', \tag{2.12}$$

where ω and γ are correlation coefficients, P' is the perturbation of the spatially distributed colloid deposition rate constant, and Y' is the perturbation of the hydraulic conductivity field. Note that $\langle P'=0\rangle$ and $\langle Y'=0\rangle$. When $\omega=0$ and $\gamma>0$, P and Y are perfectly positively correlated; when $\omega=0$ and $\gamma<0$, P and Y are perfectly negatively correlated; and when $\omega\neq 0$, P and Y are not perfectly correlated. For Brownian colloids, $\omega=0$ and $\gamma>0$; the value of γ is chosen as $1/3$, because k_{dep} is proportional to $K^{1/3}$.

3. Numerical procedures

In this colloid transport model, the transient flow equation is coupled to the colloid transport equation. Numerical solutions can be obtained with both transient and steady state flow fields using the MCB method (Sun, 1995).

3.1. Initial and boundary conditions

The flow region in our model is a vertical rectangular domain, with the horizontal x-axis ranging from 0 to 3 m and the vertical z-axis ranging from 0 and 1 m. The four straight lines (Γ_1 on which $x=0$, Γ_2 on which $z=0$, Γ_3 on which $z=1$, and Γ_4 on which $x=3$) of the rectangular domain form the boundary Γ. The computational domain Ω is encircled by the line boundary Γ. The initial and boundary conditions for the flow equation are specified as follows:

$$h(x) = h_0 \quad \text{at} \quad t = 0, \tag{3.1a}$$

$$h(0,z,t) = h_1 \quad \text{for} \quad t > 0, (0,z) \in \Gamma_1, \tag{3.1b}$$

$$\left.\frac{\partial h(x,z,t)}{\partial z}\right|_{z=0} = 0 \quad \text{for} \quad t > 0, (x,0) \in \Gamma_2, \tag{3.1c}$$

$$\left.\frac{\partial h(x,z,t)}{\partial z}\right|_{z=1} = 0 \quad \text{for} \quad t > 0, (x,1) \in \Gamma_3, \tag{3.1d}$$

$$h(3,z,t) = h_2 \quad \text{for} \quad t > 0, (3,z) \in \Gamma_4, \tag{3.1e}$$

where $\Gamma = \Gamma_1 \cup \Gamma_2 \cup \Gamma_3 \cup \Gamma_4$, and h_1 and h_2 are fixed values of hydraulic heads on the boundaries. The steady state flow field is generated by using the transient flow equation for sufficiently long time.

The initial and boundary conditions for the colloid transport equation are specified as follows. Initially the porous medium has no deposited colloids (i.e., zero surface coverage, $\theta_f = \theta_u = 0$). At the four boundaries of the rectangular domain (Γ_1, Γ_2, Γ_3, and Γ_4), zero dispersive flux boundary conditions are specified. Furthermore, a given concentration of colloids is injected into the domain at $t > 0$. The type of colloid injection can be classified as pulse injection or continuous injection, depending on the duration of the injection. The mode of injection can be characterized as point injection or line injection based on the number and locations of injection wells. The injection is set as the boundary condition for the colloid concentration.

3.2. Multiple cell balance algorithm

When physical and chemical heterogeneities are involved, there is no analytical solution for the coupled flow and colloid transport problem. In this section, we will develop a numerical method for solving this problem which is an extension of the MCB method originally developed by Sun and Yeh (1983).

The following notations are used to derive the MCB solution:

$$\gamma = \pi a_p^2 / f, \tag{3.2a}$$

$$K_a(\theta_f, \theta_u) = \pi a_p^2 \left[k_{dep,f} B(\theta_f)\, \lambda + k_{dep,u} B(\theta_u)(l - \lambda) \right], \tag{3.2b}$$

$$K_r(\theta_f, \theta_u) = k_{det,f} \theta_f \lambda + k_{det,u} \theta_u (1 - \lambda). \tag{3.2c}$$

In writing (3.2c), we assume that the dynamic release function is unity; i.e., the release process follows first-order kinetics. The governing colloid transport equation can then be written as

$$\frac{\partial n}{\partial t} = \nabla \cdot (\mathbf{D}\nabla n) - \nabla \cdot (\mathbf{V}n) - \frac{K_a(\theta_f, \theta_u)}{\gamma} n + \frac{K_r(\theta_f, \theta_u)}{\gamma}. \tag{3.3}$$

Integrating (3.3) for our two-dimensional problem and applying Green's formula, we obtain

$$\int_{(\Gamma)} \left[\left(D_{xx}\frac{\partial n}{\partial x} + D_{xz}\frac{\partial n}{\partial z} \right) \mathrm{d}z - \left(D_{xz}\frac{\partial n}{\partial x} + D_{zz}\frac{\partial n}{\partial z} \right) \mathrm{d}x \right] + \int_{(\Gamma)} n(V_z \mathrm{d}x - V_x \mathrm{d}z)$$
$$= \int\int_{(\Omega)} \left[\frac{\partial n}{\partial t} + \frac{K_a(\theta_f, \theta_u)}{\gamma} n - \frac{K_r(\theta_f, \theta_u)}{\gamma} \right] \mathrm{d}x\mathrm{d}z. \tag{3.4}$$

The first step of the MCB algorithm is to partition the domain Ω (defined in Section 3.1) into a triangular net. Considering an arbitrary element (e), we number the nodes by i, j, k, with the coordinates (x_i, z_i), (x_j, z_j), (x_k, z_k) (Fig. 1). The colloid number

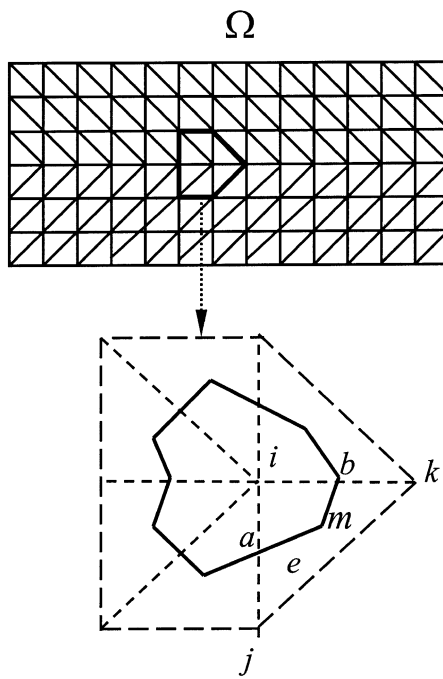

Fig. 1. The computational domain Ω (top) and the exclusive subdomain for node i (bottom) in the MCB method. The computational domain is divided into a triangular net. The arbitrary element (e) is the triangle Δijk, with its center at point m. The points a and b are the midpoints of the sides ij and ik. By connecting m, a, b, and the centers and midpoints of the other adjacent triangles, the exclusive subdomain of node i is formed as shown by the area enclosed by the solid lines.

concentration in this element, denoted by $n(x,z,t)$, can be approximated by a linear interpolation of its nodal values:

$$n(x,z,t) = \phi_i(x,z)\,n_i(t) + \phi_j(x,z)\,n_j(t) + \phi_k(x,z)\,n_k(t), \quad (x,z) \in (e), \tag{3.5}$$

where the interpolation function is

$$\phi_l(x,z) = \frac{1}{2\Delta_e}(a_l + b_l x + c_l z); \quad l = i,j,k. \tag{3.6}$$

Here, Δ_e is the area of a triangular element (e), and a_l, b_l, and c_l are coefficients which can be calculated on the coordinates of nodes i, j, k (Sun, 1995). The following expressions can then be written for the element (e):

$$\frac{\partial n}{\partial x} = \frac{1}{2\Delta_e}(b_i n_i + b_j n_j + b_k n_k), \tag{3.7a}$$

$$\frac{\partial n}{\partial z} = \frac{1}{2\Delta_e}(c_i n_i + c_j n_j + c_k n_k), \tag{3.7b}$$

$$\frac{\partial n}{\partial t} = \phi_i \frac{\partial n_i}{\partial t} + \phi_j \frac{\partial n_j}{\partial t} + \phi_k \frac{\partial n_k}{\partial t}. \tag{3.7c}$$

The hydraulic head (h) and velocity components V_x and V_z, can also be represented by the same linear interpolation functions defined in Eq. (3.5).

The second step is to form a subdomain surrounding the node i by linking up the center and midpoints of the sides of each triangle (Fig. 1). This area is called the *exclusive subdomain* of node i. Local mass balance requires that Eq. (3.4) be satisfied in the exclusive subdomain as well.

In the third step, taking into account the boundary conditions and substituting the relevant Eqs. (3.5, 3.7a, 3.7b, 3.7c) into Eq. (3.4) with respect to the domain Ω for every unknown concentration node, we obtain a system of ordinary differential equations (ODEs)

$$[A']n + [B']\frac{\mathrm{d}n}{\mathrm{d}t} + F' = 0, \tag{3.8}$$

where $F' = [(K_{\mathrm{r},i}(\theta_\mathrm{f},\theta_\mathrm{u})/\gamma)(1/n_0)]S_i$, with S_i being the area of the exclusive subdomain. The term in brackets accounts for the colloid release process, and A' and B' are coefficients with A' containing the colloid deposition term $[(K_{\mathrm{a},i}(\theta_\mathrm{f},\theta_\mathrm{u}))/\gamma]$.

The fourth step is to solve the system of ODEs numerically by using the backward Euler method. Because the transport equation and the surface coverage rate equation are coupled, an iterative scheme is needed. A simple iteration approach is adopted to obtain the colloid number concentration at each node. First, the unknown colloid number concentration is calculated based on the surface coverage at the old time level. Then the new surface coverage rate is obtained according to the calculated colloid number

concentration. The surface coverage can be calculated from the surface coverage rate by applying a first-order finite difference scheme

$$\theta_l^{\text{new}} = \theta_l^{\text{old}} + \frac{\partial \theta_l}{\partial t}\Delta t, \tag{3.9}$$

where l represents the subscripts f or u, which denote the favorable and unfavorable surface fractions, respectively. The surface coverage rate is determined from

$$\frac{\partial \theta_l}{\partial t} = \pi a_{\text{p}}^2 k_{\text{dep},l} B\left(\theta_l^{\text{old}}\right) n^{\text{cal}} - k_{\text{det,l}} \theta_l^{\text{old}}, \tag{3.10}$$

where n^{cal} is the calculated colloid number concentration. The new surface coverage is then compared with its old value. If the specified criterion for convergence is not satisfied, the new surface coverage rate is recorded as the old value and substituted into the transport equation to start another iteration between the transport equation and the surface coverage rate equation. The iteration stops when the convergence criterion is satisfied for every node in the entire domain Ω.

To obtain an accurate numerical solution, both numerical dispersion and oscillations are controlled simultaneously in the numerical code. The local Peclet number $\Delta xV/D$ was set to less than 1 to control numerical dispersion. When the fluid velocity was too high, the upstream scheme was included in the MCB code through a weighting parameter to minimize oscillation errors. The Courant number, defined as the product of interstitial velocity and time step size divided by the spatial step size in the flow direction, was also set to less than 1 so that the average displacement of fluid is less than the length of one grid space in one time step.

3.3. Validation of the numerical code

To validate the MCB code for colloid transport, the analytical solution derived by Lapidus and Amundson (1952) for the one-dimensional solute transport problem with finite rates of sorption (k_1) and desorption (k_2) was compared with our numerical solution for the following problem:

$$\frac{\partial C}{\partial t} = D_{\text{L}} \frac{\partial^2 C}{\partial x^2} - V\frac{\partial C}{\partial x} - \frac{1}{\beta}\frac{\partial S}{\partial t}, \tag{3.11a}$$

$$\frac{\partial S}{\partial t} = k_1 C - k_2 S, \tag{3.11b}$$

where $\beta = \varepsilon/\rho_{\text{b}}$. As with Eq. (2.7), these equations can be expressed in terms of n and θ. The rate constants k_1 and k_2, and the parameter β then become

$$k_1 = \left[\lambda k_{\text{dep,f}} + (1-\lambda) k_{\text{dep,u}}\right] f, \tag{3.12a}$$

$$k_2 = (1-\lambda) k_{\text{det,u}} f/\left(\pi a_{\text{p}}^2 n_0\right), \tag{3.12b}$$

$$\beta = 1.0. \tag{3.12c}$$

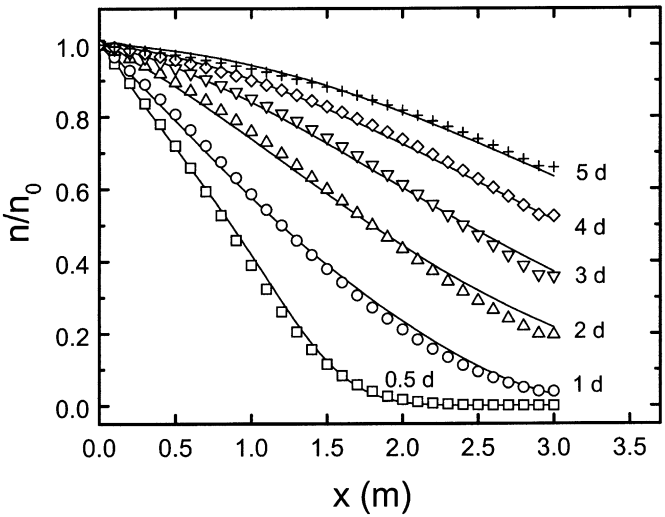

Fig. 2. Comparison of normalized colloid concentration profiles as a function of the longitudinal distance x based on the MCB numerical solution (symbols) with the analytical solution, Eq. (3.13) (solid lines). The parameters used in the calculations are: Darcy's velocity $q = 1.0$ m/day; $\alpha_L = 0.05$ m, $D_d = 6.0\times10^{-7}$ m^2/s, $\lambda = 0.01$, $k_{dep,f} = 6.5\times10^{-3}$ m/day, $k_{dep,u} = 6.5\times10^{-6}$ m/day, $k_{det,u} = 5\times10^{-4}$ d^{-1}, $d_p = 300$ nm, $d_c = 0.3$ mm, $\varepsilon = 0.4$, $n_0 = 2.8\times10^{14}$ m^{-3}. Observation times (in days) are indicated next to each curve.

The initial concentration is set to zero, the concentration at the inlet boundary is given as a constant n_0, and the dispersive colloid flux is set to zero at the outlet boundary. The analytical solution of Lapidus and Amundson (1952) is given by

$$\frac{n}{n_0} = e^{\frac{Vx}{2D}}\left[F(t) + k_2\int_0^t F(\tau)d\tau\right], \tag{3.13}$$

where

$$F(t) = e^{-k_2 t}\int_0^t I_0\left[2\sqrt{\frac{k_1 k_2 \tau}{\beta}(t-\tau)}\right]\frac{x}{2\sqrt{\pi D\tau^3}}e^{-\frac{x}{4D\tau}-\tau d}d\tau, \tag{3.14}$$

and

$$d = \frac{V^2}{4D} + \frac{k_1}{\beta} - k_2. \tag{3.15}$$

As shown in Fig. 2, the numerical results obtained from the MCB code are in very close agreement with the analytical solution.

4. Results and discussion

The newly developed two-dimensional colloidal transport model was used to conduct a numerical investigation of colloidal transport in physically and geochemically hetero-

geneous porous media. We first illustrate the effect of key model parameters on the general colloid transport behavior. This is followed by a systematic investigation of colloid transport in layered as well as randomly heterogeneous subsurface porous media.

4.1. Influence of key model parameters

The basic values of the model parameters and the range of their variation during the numerical investigation are listed in Table 1. The range of parameter values covers possible scenarios of colloid transport in sandy aquifers, such as the glacial outwash sandy aquifer on Cape Cod, MA, which has been used extensively in field investigations (LeBlanc et al., 1991; Garabedian et al., 1991; Hess et al., 1992; Gelhar et al., 1992; Sun, 1995; Harvey et al., 1989; Ryan et al., 1999). Colloidal particles are introduced at the boundary $x = 0$ as a pulse injection with a duration of 0.5 day. The results (Fig. 3) are presented as relative colloid concentration n/n_0 along the flow direction x at a certain observation time ($t = 0.75$ day).

Table 1
Basic values of parameters used in the colloid transport model predictions

Parameter	Basic value
Hydrologic parameters	
Hydraulic gradient, ∇h	0.01
Hydraulic conductivity, K (m/day)	100
Specific storage, S_S	0.0001
Longitudinal dispersivity, α_L (m)	0.05
Ratio of dispersivities, α_L / α_T	5:1
Porosity, ε	0.4
Transport parameters	
Grain diameter, d_c (mm)	0.3
Specific surface area,[a] f (m^2/m^3)	3×10^4
Particle radius, a_p (μm)	0.15
Medium bulk density, ρ_b (g/cm^3)	2.5
Initial particle concentration, C_0 (mg/l)	10
Initial particle number concentration, n_0 (m^{-3})	2.8×10^{14}
Collision efficiency (with unfavorable surfaces), α_u	10^{-3}
Favorable single collector efficiency,[b] η_0	0.0259
Patchwise heterogeneity parameter, λ	0.001 (0.1%)
Unfavorable particle deposition rate,[c] $k_{dep,u}$ (m/day)	6.5×10^{-6}
Favorable particle deposition rate,[d] $k_{dep,f}$ (m/day)	6.5×10^{-3}
Detachment rate from unfavorable surface, $k_{det,u}$ (h^{-1})	0.0
Detachment rate from favorable surface, $k_{det,f}$ (h^{-1})	0.0
Maximum attainable surface coverage,[e] θ_{max}	0.2

[a] Determined from $6(1-\varepsilon)/(\varepsilon d_c)$.
[b] Calculated numerically as described in Song and Elimelech (1994).
[c] Determined from Eq. (2.10), using the values of η_0 and α_u above.
[d] Determined from Eq. (2.10), using the value of η_0 above and collision efficiency of 1 (favorable).
[e] Typical value based on Johnson et al. (1996).

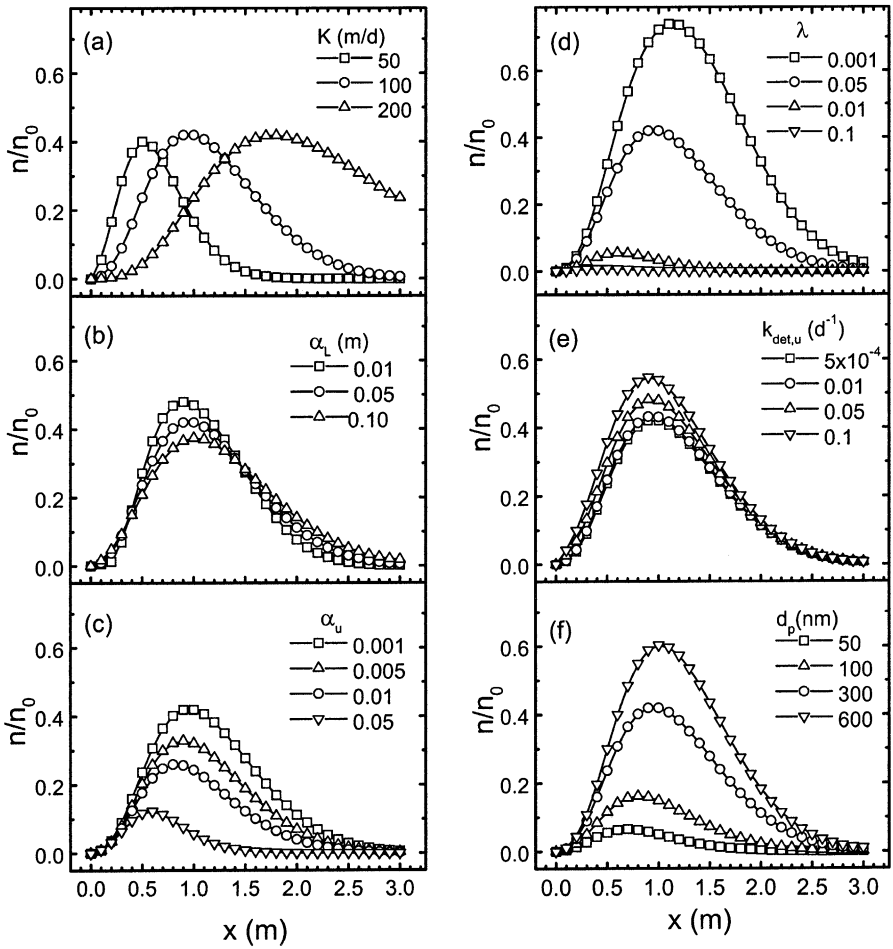

Fig. 3. Effect of key model parameters on colloid transport along x (at $z = 0.5$ m) in physically homogeneous porous media. The following effects are shown: (a) hydraulic conductivity, (b) longitudinal dispersivity, (c) collision (attachment) efficiency (unfavorable deposition rate), (d) geochemical heterogeneity, (e) release rate from unfavorable surface fraction; and (f) particle size (diameter). Parameter values are indicated in each figure. The basic parameters and variables used in the numerical calculations are presented in Table 1.

4.1.1. Hydraulic conductivity and hydrodynamic dispersivities

Under the examined conditions, an increase in hydraulic conductivity results in enhanced colloid migration and a wider spreading of the colloid concentration profiles (Fig. 3a). With a constant hydraulic head gradient, a greater hydraulic conductivity results in a greater flow velocity so that the colloid advection velocity increases. Because the colloid dispersion coefficient is proportional to the colloid advection velocity, spreading of the colloid plume also increases as the hydraulic conductivity is increased. In addition, the capture (removal) of colloids traveling through the porous

medium decreases with increasing flow velocity, resulting in a slightly less attenuated colloid concentration profile.

Hydrodynamic dispersion is also controlled by the longitudinal and transverse dispersivities (Eq. (2.6)). The ratio of longitudinal dispersivity to transverse dispersivity is typically in the range of 5–20 (Sun, 1995). We assumed a ratio of 5 and investigated the effect of varying the longitudinal dispersivity. Because the longitudinal dispersivity is scale-dependent, and our problem is of local scale (ca. 3 m), only a narrow range of values was selected for the longitudinal dispersivity. The results (Fig. 3b) show that small changes in longitudinal dispersivity lead to relatively large changes in the colloid concentration profiles.

4.1.2. Particle deposition rate and attachment (collision) efficiency

To investigate the effect of particle deposition rate on colloid transport behavior, a constant geochemical heterogeneity ($\lambda = 0.01$) was assumed. We fixed the favorable particle deposition rate coefficient and adjusted the unfavorable deposition rate by choosing different values for the collision efficiency of the unfavorable surface fraction α_u. The results (Fig. 3c) show that particle deposition rate can substantially affect the colloid concentration profile. As the collision efficiency α_u increases, the colloid deposition rate on the unfavorable surface fraction increases, and less colloids can be detected in the aqueous phase. The magnitude of the collision efficiency α_u reflects the effect of changes in the solution chemical composition (Elimelech and O'Melia, 1990).

4.1.3. Geochemical heterogeneity

By fixing the particle deposition rate coefficients $k_{dep,f}$ and $k_{dep,u}$, the overall particle deposition rate can be controlled by the geochemical heterogeneity parameter λ. The marked effect of geochemical heterogeneity on colloidal transport is illustrated in Fig. 3d. An increase in geochemical heterogeneity results in an increased overall colloid deposition rate and a reduced concentration of colloids in bulk solution. For the conditions investigated in Fig. 3d, a substantial geochemical heterogeneity of subsurface porous media ($> 10\%$) may result in nearly complete immobilization of colloidal particles as shown by the flat, attenuated colloid concentration profile.

4.1.4. Particle release rate

The colloidal transport model assumes that particle deposition onto the favorable surface fraction is irreversible; hence, the colloid release rate from the favorable surface fraction is zero. This assumption has been confirmed in particle deposition studies involving oppositely charged particles and collector surfaces (Ryan and Elimelech, 1996). On the other hand, in particle deposition studies involving similarly charged particles and collector surfaces, a finite rate of colloid release can be detected (Meinders et al., 1992; Johnson et al., 1996). Hence, we investigated the effect of colloid release rate from the unfavorable surface fraction on the colloid concentration profile as shown in Fig. 3e. The results demonstrate that larger release rate coefficients result in increased colloid concentration in the aqueous phase, whereas smaller release rate coefficients have negligible effect on the colloid concentration profile. Since the colloid release rate depends on the concentration of deposited particles (first-order kinetics), the effect of

colloid release on the colloid concentration profile depends on the overall colloid deposition rate onto the unfavorable surface fraction.

4.1.5. Particle size

Fig. 3f demonstrates that the model solution is very sensitive to particle size. Particle size influences colloidal transport mainly through its effect on colloid deposition rate. As expected for the deposition of Brownian particles, which is controlled by a convective-diffusion mechanism, the deposition rate becomes smaller as particle size increases. Consequently, larger particles migrate faster in the porous medium and their concentration in the liquid phase is greater than that of smaller particles.

4.2. Colloid transport in layered heterogeneous porous media

The porous medium was divided into three horizontal layers parallel to the flow direction. The layers are denoted as layer I (0–0.3 m), layer II (0.3–0.7 m), and layer III (0.7–1.0 m) from bottom to top. Layers I and III were assigned the same heterogeneity parameter values, whereas a different parameter value was assigned to the middle layer II. The colloid suspension was assumed to be fed continuously (line injection) into the porous medium at the inlet boundary ($x = 0$), with 11 injection points set at 0.1 m intervals along the z-direction. Observations of the normalized concentration profiles over the entire two-dimensional porous medium domain are presented for $t = 0.75$ day. The physical and geochemical heterogeneity parameter values used in the numerical investigation (represented by K and λ, respectively) were comparable to those reported for the Cape Cod sandy aquifer (Harvey et al., 1989; Hess et al., 1992; Ryan et al., 1999).

The effect of layered–distributed physical heterogeneity on colloid transport is illustrated in Fig. 4. The hydraulic conductivity of the middle layer (layer II) of the porous medium is twice as large as the hydraulic conductivity in the layers above and

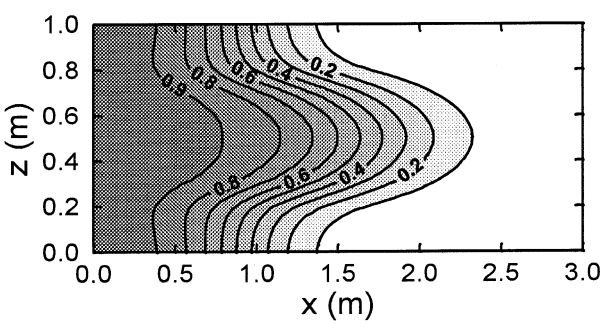

Fig. 4. Effect of layered porous medium physical heterogeneity on colloid transport. The contours describe the residual particle concentration (n/n_0) at an observation time of 0.75 day. The central layer (z between 0.3 and 0.7 m) has $K = 100$ m/day and the layers above (z between 0.7 and 1.0 m) and below (z between 0 and 0.3 m) are with $K = 50$ m/day. Colloids are continuously injected along the depth (z-axis) on the left boundary of the porous medium ($x = 0$). The basic parameters and variables used in the numerical calculations are presented in Table 1.

below. Therefore, the fluid in the central layer flows faster than the other two layers, and most of the colloids migrate with the flow through the more permeable layer. This example points out to the paramount importance of preferential flow paths in colloid transport, which can be significantly important in colloid-facilitated transport of contaminants (Ibaraki and Sudicky, 1995a,b).

Because transverse dispersion reduces the amount of colloids passing through the preferential flow path, the role of longitudinal and transverse dispersivities was also investigated. Two different ratios of longitudinal to the transverse dispersivities (1 and 10) were studied, as shown in Fig. 5. When the transverse dispersion is relatively large ($\alpha_L/\alpha_T = 1$), the extent of preferential flow in the middle (most permeable) layer of the porous medium is reduced (Fig. 5a). However, when the transverse dispersion is relatively small ($\alpha_L/\alpha_T = 10$), the preferential transport of colloids in the middle layer of the porous medium is enhanced (Fig. 5b). The results demonstrate that hydrodynamic dispersion can influence colloid transport in layered heterogeneous porous media, but the effect is not strong enough to explain the preferential transport of colloidal particles.

The effect of layered geochemical heterogeneity on colloid transport in physically homogeneous (constant hydraulic conductivity) subsurface porous medium is shown in Fig. 6. The central layer has a very small value of geochemical heterogeneity ($\lambda = 0.001$), whereas the upper and lower layers have much higher values ($\lambda = 0.025$). The results clearly show that the increased deposition rate of colloidal particles onto the favorable surface fractions of the more heterogeneous (lower and upper) layers can result in

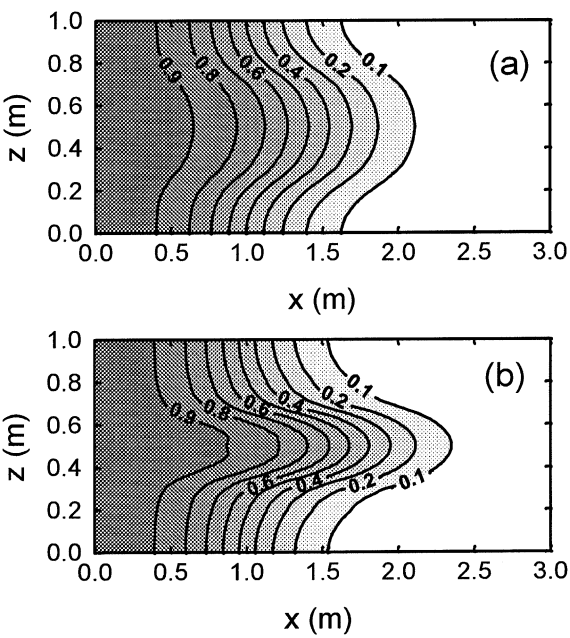

Fig. 5. Effect of the ratio of α_L/α_T on the preferential flow of colloids caused by layered physical heterogeneity of porous media: (a) $\alpha_L/\alpha_T = 1$ and (b) $\alpha_L/\alpha_T = 10$. All other conditions are the same as in Fig. 4.

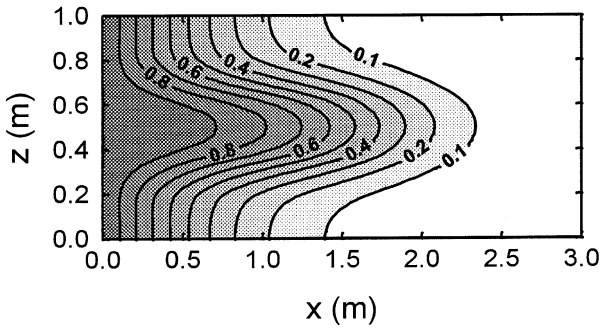

Fig. 6. Preferential flow of colloids caused by layered geochemical heterogeneity in an otherwise physically homogeneous porous medium ($K = 100$ m/day throughout the entire domain). The central layer (z between 0.3 and 0.7 m) has $\lambda = 0.001$ and the layers above (z between 0.7 and 1.0 m) and below (z between 0 and 0.3 m) are with $\lambda = 0.025$. Colloids are continuously injected along the depth (z-axis) on the left boundary of the porous medium ($x = 0$). The basic parameters and variables used in the numerical calculations are presented in Table 1.

preferential flow of colloidal particles through the middle layer, similar to what is observed for layered, physically heterogeneous porous media (Fig. 4).

Because subsurface porous media are physically as well as geochemically heterogeneous, it is of great interest to investigate the combined effect of layered physical and geochemical heterogeneities. For the layered physically heterogeneous porous medium shown in Fig. 4 (i.e., $K = 50$, 100, and 50 m/day from top to bottom), we assumed that the geochemical heterogeneity is layered distributed as well. Fig. 7a illustrates the results when the central layer has a larger λ (0.025) compared to the layers above and below ($\lambda = 0.001$). It is interesting to note that for these conditions the preferential flow path (initially caused by the higher hydraulic conductivity, Fig. 4) disappears due to the geochemical heterogeneity. On the other hand, the preferential flow path is enhanced when the middle layer has a smaller λ (0.001) than the layers above and below ($\lambda = 0.025$), as shown in Fig. 7b. The results clearly demonstrate that layered geochemical heterogeneity can significantly alter the preferential transport of colloidal particles caused by heterogeneous flow field. Hence, consideration of physical or geochemical heterogeneity alone in colloidal transport models may result in erroneous results.

4.3. Colloid transport in randomly heterogeneous porous media

Colloid transport in randomly heterogeneous porous media is investigated in this section. The numerical investigation is carried out for a point injection (at $x = 0.5$ m, $z = 0.5$ m) with a pulse duration of 0.1 day. Results are presented as snapshots of colloid concentration in the porous medium at $t = 0.5$ day.

4.3.1. Colloid transport in randomly physically heterogeneous porous media

Freeze (1975) pointed out that hydraulic conductivity variations in aquifers are typically lognormally distributed with a standard deviation (in log base 10 units) ranging from 0.2 to 2.0. Since then, several field measurements have confirmed this observation.

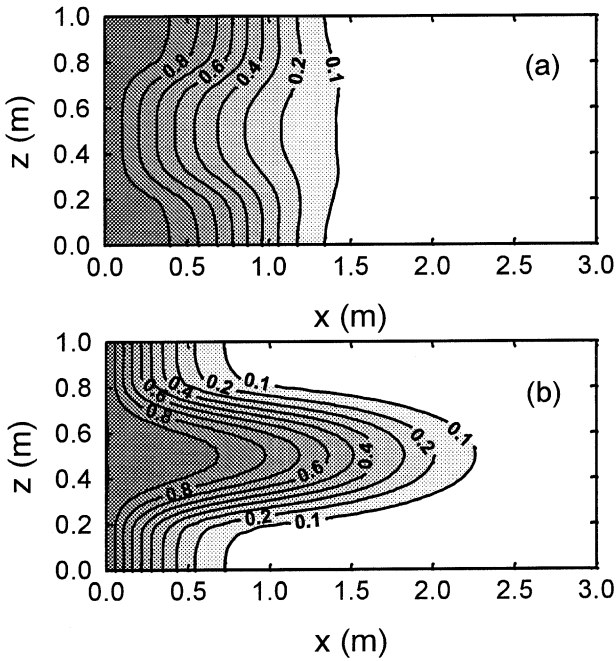

Fig. 7. Effect of porous medium layered geochemical heterogeneity on the preferential flow of colloids caused by the porous medium physical heterogeneity. (a) The central layer has $K = 100$ m/day and $\lambda = 0.025$; the upper and lower layers have $K = 50$ m/day and $\lambda = 0.001$. (b) The central layer has $K = 100$ m/day and $\lambda = 0.001$; the upper and lower layers have $K = 50$ m/day and $\lambda = 0.025$. All other conditions are the same as in Fig. 4.

For instance, it was reported that the mean hydraulic conductivity K for the Borden site is 0.0072 cm/s with the variance of ln K being 0.29 (Sudicky, 1986). Hufschmied (1986) reported that the mean value of K is 0.36 cm/s for the Aefligen site with a variance of $\ln K$ of 2.15. The integral scales in the x, y (horizontal), and z (vertical) directions were reported to be 0.29, 2.8, and 0.12 m, respectively, for the Borden site (Sudicky, 1986); 0.26, 5.1, and 0.26 m, respectively, for the Cape Cod site (Hess, 1989); and 0.031, 3.0, and 0.91 m, respectively, for the Twin Lakes site (Moltyaner, 1986).

In our study, the mean value of K was set at 0.116 cm/s (100 m/day), the variance of ln K was set at 0.24 or 2.4, and the integral scale of the vertical porous medium was set at 0.5 m. The random field of hydraulic conductivity was generated numerically as outlined earlier in this paper and incorporated into the MCB code of colloid transport. Similar variance values were used to generate the random field of the particle deposition rates. The mean values of the deposition rate coefficients were set at 6.5×10^{-3} m/day for the favorable surface fraction and at 6.5×10^{-6} m/day for the unfavorable surface fraction. Note that the latter corresponds to $\alpha_u = 10^{-3}$.

Realizations of the random fields of hydraulic conductivity with two different variance values of ln K (0.24 and 2.4) are shown in Fig. 8. Fig. 9 presents the

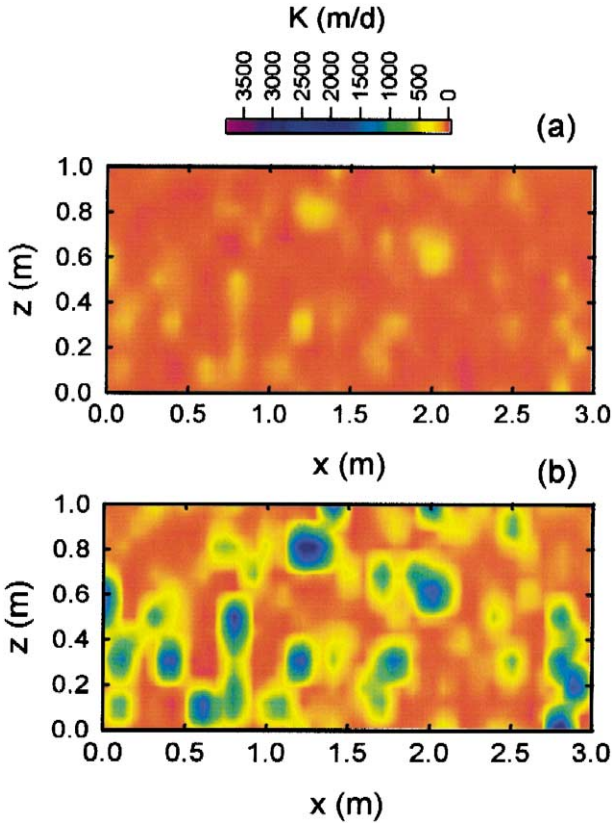

Fig. 8. Realizations of random hydraulic conductivity fields. (a) Mean $E(K) = 100$ m/day and variance $\mathrm{Var}(\ln K) = 0.24$. (b) Mean $E(K) = 100$ m/day and variance $\mathrm{Var}(\ln K) = 2.4$.

corresponding hydraulic head distributions and non-dimensional colloid concentration profiles in the randomly physically heterogeneous porous media; the results for physically homogeneous porous media are presented as well. Compared to the physically homogeneous case (Fig. 9a), random fields of $\ln K$ result in obvious irregular hydraulic head distributions (Fig. 9b,c). The irregularity of the hydraulic head distributions increases with the variance of $\ln K$. A similar trend can be observed in the colloid concentration profiles. When the variance of $\ln K$ is small, the colloid concentration profile (Fig. 9e) is only slightly different than the homogeneous case (Fig. 9d). However, a very irregular shape of the concentration profile (Fig. 9f) can be seen when the variance of $\ln K$ is large. The results clearly demonstrate that a random physical heterogeneity of porous media results in a random behavior of colloid transport as well.

4.3.2. Colloid transport in randomly geochemically heterogeneous porous media

Because of lack of field measurements on random geochemical heterogeneity of subsurface porous media, we conducted a preliminary numerical investigation on the

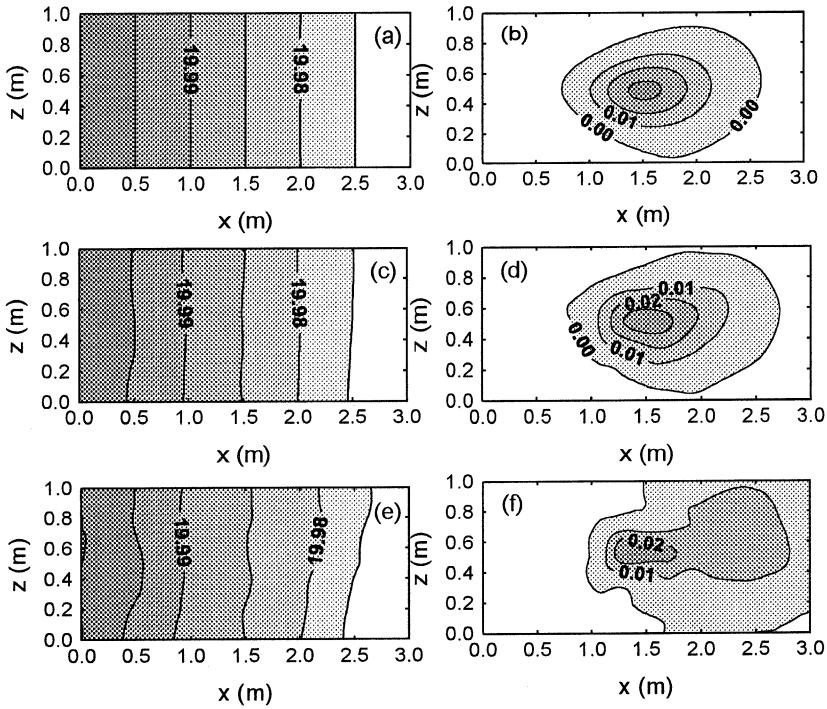

Fig. 9. Hydraulic head distributions (left) and the corresponding normalized colloid concentration profiles (right) in homogeneous (top) and randomly physically heterogeneous porous media. In all the figures shown, the mean value of the hydraulic conductivity $E(K)$ is 100 m/day. The figures are for the following degrees of heterogeneity: (a, b) physically homogeneous porous medium; (c, d) variance $\mathrm{Var}(\ln K) = 0.24$; (e, f) variance $\mathrm{Var}(\ln K) = 2.4$. The results are for point injection (at $x = 0.5$ m and $z = 0.5$ m) with a duration of 0.1 day. The observation time is 0.5 day. The other parameters and variables used in the numerical calculations are presented in Table 1.

sensitivity of the colloid transport behavior to the parameters characterizing the geochemical heterogeneity. Results indicated that the mean value of geochemical heterogeneity has to be large enough ($\lambda = 0.01$) to show the effect of its spatial distribution on the colloid concentration profiles. When the mean value of λ is as small as 0.001, which may be a reasonable value for sandy aquifers with negligible iron oxyhydroxide coatings or laboratory experiments with clean quartz sand, the distribution of λ apparently does not affect the colloid transport behavior, even when λ is assumed to have a lognormal distribution with a rather large variance. Therefore, a mean value of $\lambda = 0.01$ was chosen to carry out the rest of the numerical investigation. This value may be reasonable for the upper limit of geochemical heterogeneity of ferric oxyhydroxide coated sand aquifers (Heron et al., 1994; Coston et al., 1995, Ryan et al., 1999). It was also found that a lognormally distributed field of λ with a relatively small variance does not affect the particle concentration profiles; therefore, a variance of ln λ as large as 2.0 was chosen.

Realizations of the random fields of λ are shown are Fig. 10. For a normal distribution, a standard deviation as large as 0.005 was chosen. Of the simulated λ values, about 2.5% are negative; these negative values are set to zero in the spatial distribution. Fig. 10a shows that the value of λ is mostly distributed from 0.0 to 0.02. For a lognormal distribution, the variance of $\ln\lambda$ was set at 2.0. We truncated about 2 percent values which are larger than 1.0. The value of λ varies mainly between 0.001 to 0.2 and some values of λ can even reach 1.0 (Fig. 10b).

The normalized colloid concentration profiles for the two different geochemical heterogeneity fields are compared with the case of a constant λ in Fig. 11. The normally distributed random field of geochemical heterogeneity apparently does not affect the colloid concentration profiles (Fig. 11b). A lognormal field of geochemical heterogeneity with a very large variance (Fig. 11c) developed only a slight irregularity in the concentration profile. These results suggest the effect of a random field of geochemical heterogeneity on colloidal transport is not as strong as that of random physical

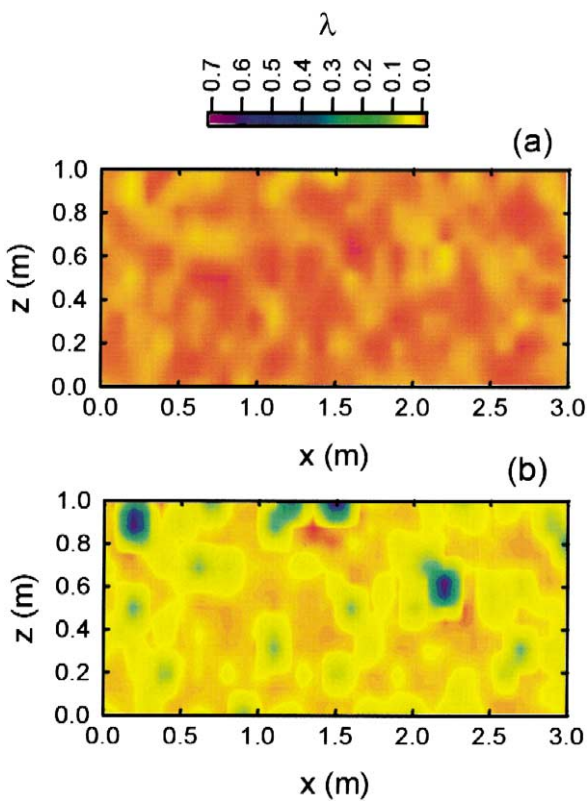

Fig. 10. Realizations and value distributions of random geochemical heterogeneity fields: (a) normal distribution with mean $E(\lambda) = 0.01$ and standard deviation $\sigma(\lambda) = 0.005$, and (b) lognormal distribution with a mean $E(\lambda) = 0.01$ and variance $\mathrm{Var}(\ln\lambda) = 2.0$.

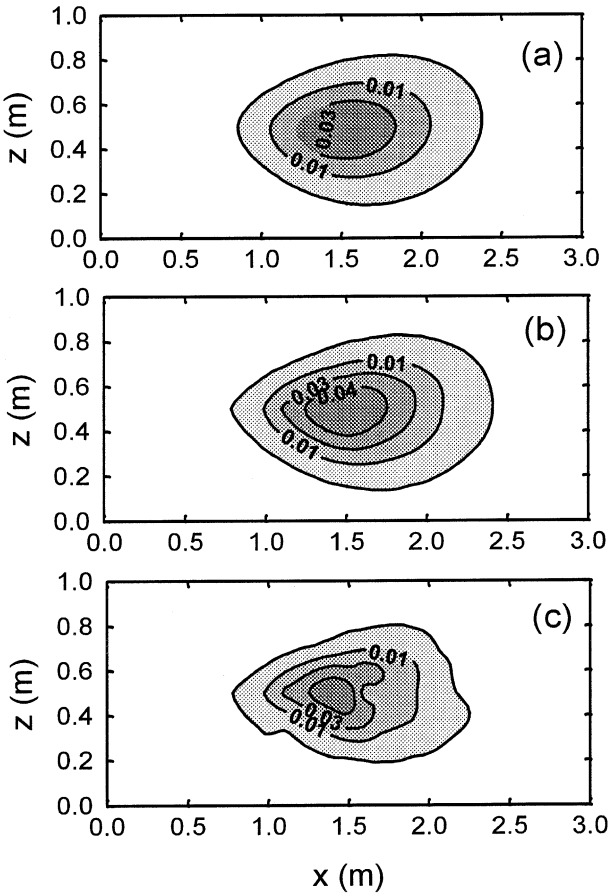

Fig. 11. Effect of random geochemical heterogeneity on colloid transport behavior. The contours of the normalized colloid concentration profiles are for an observation time of 0.5 day in response to a point injection (at $x = 0.5$ m and $z = 0.5$ m) with a duration of 0.1 day. The figures are for the following degrees of heterogeneity: (a) constant geochemical heterogeneity, $\lambda = 0.01$; (b) normally distributed geochemically heterogeneity with $E(\lambda) = 0.01$ and $\sigma(\lambda) = 0.005$; (c) lognormally distributed geochemical heterogeneity with $E(\lambda) = 0.01$ and $\mathrm{Var}(\ln\lambda) = 2.0$. The other parameters and variables used in the numerical calculations are presented in Table 1.

heterogeneity. Thus, the mean value of geochemical heterogeneity is more important than its distribution in modeling colloid transport in heterogeneous porous media.

5. Concluding remarks

A two-dimensional colloidal transport model considering the geochemical and physical heterogeneity of porous media as well as the dynamic aspects of particle deposition and release has been presented. Simulations of colloid transport in layered heteroge-

neous porous media indicate that both physical and geochemical heterogeneities play an important role in colloid transport. Both types of layered heterogeneity can result in preferential flow of colloidal particles. The combined effect of layered physical and geochemical heterogeneities, however, may enhance or reduce preferential flow of colloids.

A random distribution of hydraulic conductivity results in a random flow field and an irregularly distributed colloid concentration profile in the porous medium. Compared with random physical heterogeneity, the effect of random patchwise geochemical heterogeneity on colloid transport behavior is not significant. It is mostly the mean value of geochemical heterogeneity rather than its distribution that governs the colloid transport behavior.

The model results have direct implications for colloid-facilitated transport of contaminants in groundwater. We expect a limited potential for colloid-facilitated transport of contaminants in surficial aquifers with porous matrix having Fe oxyhydroxide coatings because of extensive colloid deposition. On the other hand, subsurface environments with physical heterogeneities in the form of preferential flow paths may result in extensive colloid transport and hence have the potential for colloid-facilitated contaminant transport.

Acknowledgements

The authors acknowledge the support of EPA (cooperative agreement CR824593-01 with R.S. Kerr Laboratory) and the US National Science Foundation (Grants EAR-9418472 and BES-9705717).

References

Abdel-Salam, A., Chrysikopoulos, C.V., 1995. Modeling of colloid and colloid-facilitated contaminant transport in a two-dimensional fracture with spatially variable aperture. Transp. Porous Media 20, 197–221.

Bear, J., 1972. Dynamics of Fluids in Porous Media. Dover Publications, New York.

Black, T.C., Freyberg, D.L., 1987. Stochastic modeling of vertically averaged concentration uncertainty in a perfectly stratified aquifer. Water Resour. Res. 23, 997–1004.

Bosma, W.J., van der Zee, S.E.A.T.M., 1993. Transport of reacting solute in a one-dimensional, chemically heterogeneous porous medium. Water Resour. Res. 29 (1), 117–131.

Chrysikopoulos, C.V., Abdel-Salam, A., 1997. Modeling of colloid transport and deposition in saturated fractures. Colloids Surf., A 121, 189–202.

Chrysikopoulos, C.V., Kitanidis, P.K., Roberts, P.V., 1990. Analysis of one-dimensional solute transport through porous media with spatially variable retardation factor. Water Resour. Res. 26, 437–446.

Corapcioglu, M.Y., Jiang, S., 1993. Colloid-facilitated groundwater contaminant transport. Water Resour. Res. 29 (7), 2215–2226.

Coston, J.A., Fuller, C.C., Davis, J.A., 1995. Pb^{2+} and Zn^{2+} adsorption by a natural aluminum- and iron-bearing surfaces coating on an aquifer sand. Geochim. Cosmochim. Acta 59, 3535–3547.

Dagan, G., 1989. Flow and Transport in Porous Formations. Springer-Verlag, New York.

de Marsily, C., 1986. Quantitative Hydrology. Academic Press, San Diego.

Elimelech, M., O'Melia, C.R., 1990. Kinetics of deposition of colloidal particles in porous media. Environ. Sci. Technol. 24, 1528–1536.

Freeze, R.A., 1975. A stochastic–conceptual analysis of one-dimensional groundwater flow in nonuniform homogeneous media. Water Resour. Res. 11 (5), 725–741.

Fuhs, G.W., Chen, M., Sturman, L.S., Moore, R.S., 1985. Virus adsorption to mineral surfaces is reduced by mineral overgrowth and organic coatings. Microb. Ecol. 11, 25–39.

Garabedian, S.P., Leblanc, D.R., Gelhar, L.W., Celia, M.A., 1991. Large-scale natural gradient tracer test in sand and gravel, Cape Cod, Massachusetts: 2. Analysis of spatial moments for a nonreactive tracer. Water Resour. Res. 27, 911–924.

Gelhar, L.W., Axness, C.L., 1983. Three-dimensional stochastic analysis of macrodispersion in aquifers. Water Resour. Res. 19 (1), 161–180.

Gelhar, L.W., Welty, C., Rehfeldt, K.R., 1992. A critical review of data on field-scale dispersion in aquifers. Water Resour. Res. 28 (7), 1955–1974.

Gelhar, L.W., Gutiahr, A.L., Naff, R.L., 1979. Stochastic analysis of macrodispersion in stratified aquifer. Water Resour. Res. 15 (6), 1387–1397.

Grolimund, D., Borkovec, M., Bartmettler, K., Sticher, H., 1996. Colloid-facilitated transport of strongly sorbing contaminants in natural porous media: a laboratory column study. Environ. Sci. Technol. 30, 3118–3123.

Harvey, R.W., George, L.H., Smith, R.L., LeBlanc, D.R., 1989. Transport of microspheres and indigenous bacteria through a sandy aquifer: results of natural and forced-gradient tracer experiments. Environ. Sci. Technol. 23, 51–56.

Heron, G., Crouzet, C., Bourg, A.C.M., Christensen, T.H., 1994. Separation of Fe(II) and Fe(III) in contaminated aquifer sediments using chemical extraction techniques. Environ. Sci. Technol. 28, 1698–1705.

Hess, K.M., 1989. Use of borehole flowmeter to determine spatial heterogeneity of hydraulic conductivity and macrodispersivity in a sand and gravel aquifer, Cape Cod, Massachusetts. NWWA Conference on New Field Techniques for Qualifying the Physical and Chemical properties of Heterogeneous Aquifers. Natl. Water Well Assoc., Houston, Tex.

Hess, K.M., Wolf, S.H., Celia, M.A., 1992. Large-scale natural gradient tracer test in sand and gravel, Cape Code, Massachusetts: 3. Hydraulic conductivity variability and calculated macrodispersivities. Water Resour. Res. 28 (8), 2011–2027.

Hufschmied, P., 1986. Estimation of three-dimensional statistically anisotropic hydraulic conductivity field by means of single well pumping tests combined with flowmeter measurements. Hydrogeologie 2, 163–174.

Ibaraki, M., Sudicky, E.A., 1995a. Colloid-facilitated contaminant transport in discretely fractured porous media: 1. Numerical formulation and sensitivity analysis. Water Resour. Res. 31 (12), 2945–2960.

Ibaraki, M., Sudicky, E.A., 1995b. Colloid-facilitated contaminant transport in discretely fractured porous media: 2. Fracture network examples. Water Resour. Res. 31 (12), 2961–2969.

Johnson, P.R., Elimelech, M., 1995. Dynamics of colloid deposition in porous media: blocking based on random sequential adsorption. Langmuir 11, 801–812.

Johnson, W.P., Blue, K.A., Logan, B.E., Arnold, R.G., 1995. Modeling bacterial detachment during transport through porous media as a residence-time-dependent process. Water Resour. Res. 31 (11), 2649–2658.

Johnson, P.R., Sun, N., Elimelech, M., 1996. Colloid transport in geochemically heterogeneous porous media: modeling and measurement. Environ. Sci. Technol. 30 (11), 3284–3293.

Lapidus, L., Amundson, N.R., 1952. Mathematics of adsorption in beds: VI. The effect of longitudinal diffusion in ion exchange and chromatographic columns. J. Phys. Chem. 56, 984–988.

Leblanc, D.R., Garabedian, S.P., Hess, K.M., Gelhar, L.W., Quadri, R.D., Stollenwerk, K.G., Wood, W.W., 1991. Large-scale natural gradient tracer test in sand and gravel, Cape Cod, Massachusetts: 1. Experimental design and observed tracer movement. Water Resour. Res. 27, 895–910.

Levich, V.G., 1962. Physicochemical Hydrodynamics. Prentice-Hall, New Jersey.

Liu, H.H., Molz, F.J., 1997. Comment on "Evidence for non-Gaussian scaling behavior in heterogeneous sedimentary formations" by Scott Painter. Water Resour. Res. 33 (4), 907–908.

Mantoglou, A., Wilson, J.L., 1982. The turning bands method for simulation of random fields using line generation by a spectral method. Water Resour. Res. 18 (5), 1379–1394.

McCarthy, J.F., Zachara, J.M., 1989. Subsurface transport of contaminants. Environ. Sci. Technol. 23, 496–502.

Meinders, J.M., Noordmans, J., Busscher, H.J., 1992. Simultaneous monitoring of the adsorption and desorption of colloidal particles during deposition in a parallel plate flow chamber. J. Colloid Interface Sci. 152, 265–280.

Moltyaner, G.L., 1986. Stochastic versus deterministic: a case study. Hydrogeologie 2, 183–196.

Painter, S., 1996. Evidence for non-Gaussian scaling behavior in heterogeneous sedimentary formations. Water Resour. Res. 32 (5), 1183–1195.

Roy, S.B., Dzombak, D.A., 1998. Sorption nonequilibrium effects on colloid-enhanced transport of hydrophobic organic compounds in porous media. J. Contam. Hydrol. 30, 179–200.

Rubin, Y., 1990. Stochastic modeling of macrodispersion in heterogeneous porous media. Water Resour. Res. 26 (1), 133–141.

Ryan, J.N., Elimelech, M., 1996. Colloid mobilization and transport in groundwater. Colloid Surf. A 107, 1–52.

Ryan, J.N., Elimelech, M., Ard, R.A., Harvey, R.W., 1999. Bacteriophage PRD1 and silica colloid transport and recovery in an iron oxide-coated sand aquifer. Environ. Sci. Technol. 33 (1), 63–73.

Saiers, J.E., Hornberger, G.M., Harvey, C., 1994. Colloidal silica transport through structured, heterogeneous porous media. J. Hydrol. 163, 271–288.

Scholl, M.A., Harvey, R.W., 1992. Laboratory investigation on the role of sediment surface and groundwater chemistry in transport of bacteria through a contaminated sandy aquifer. Environ. Sci Technol. 26, 1410–1417.

Scholl, M.A., Mills, A.L., Herman, J.S., Hornberger, G.M., 1990. The influence of mineralogy and solution chemistry on the attachment of bacteria to representative aquifer materials. J. Contam. Hydrol. 6, 321–336.

Song, L., Elimelech, M., 1994. Transient deposition of colloidal particles in heterogeneous porous media. J. Colloid Interface Sci. 167, 301–313.

Song, L., Johnson, P.R., Elimelech, M., 1994. Kinetic colloid deposition onto heterogeneously charged surfaces in porous media. Environ. Sci Technol. 28 (6), 1164–1171.

Sudicky, E.A., 1986. A natural gradient experiment on solute transport in a sand aquifer: spatial variability of hydraulic conductivity and its role in the dispersion process. Water Resour. Res. 22 (13), 2069–2082.

Sun, N.-Z., 1995. Mathematical Modeling of Groundwater Pollution. Springer-Verlag, New York.

Sun, N.-Z., Yeh, W.W.-G., 1983. A proposed upstream weight numerical method for simulating pollutant transport in groundwater. Water Resour. Res. 19 (6), 1489–1500.

Tompson, A.F.B., Ababou, R., Gelhar, L.W., 1989. Implementation of the three dimensional turning bands random field generator. Water Resour. Res. 25 (10), 2227–2243.

Yates, M.V., Gerba, C.P., Kelley, L.M., 1985. Virus persistence in groundwater. Appl. Environ. Microbiol. 49, 778–781.

Zachara, J.M., Gassman, P.L., Smith, S.C., Taylor, D., 1995. Oxidation and adsorption of Co(II)EDTA2-complexes in subsurface materials with iron and manganese oxide grain coatings. Geochim. Cosmochim. Acta 59, 4449–4463.